Published OnlineFirst January 16, 2012; DOI: 10.1158/1535-7163.MCT-11-0820

*Therapeutic Discovery*

Molecular Cancer Therapeutics

# Antitumor Activity of a Novel Bispecific Antibody That Targets the ErbB2/ErbB3 Oncogenic Unit and Inhibits Heregulin-Induced Activation of ErbB3

Charlotte F. McDonagh, Alexandra Huhalov, Brian D. Harms, Sharlene Adams, Violette Paragas, Shinji Oyama, Bo Zhang, Lia Luus, Ryan Overland, Stephanie Nguyen, Jinming Gu, Neeraj Kohli, Matt Wallace, Michael J. Feldhaus, Arthur J. Kudla, Birgit Schoeberl, and Ulrik B. Nielsen

## Abstract

The prevalence of ErbB2 amplification in breast cancer has resulted in the heavy pursuit of ErbB2 as a therapeutic target. Although both the ErbB2 monoclonal antibody trastuzumab and ErbB1/ErbB2 dual kinase inhibitor lapatinib have met with success in the clinic, many patients fail to benefit. In addition, the majority of patients who initially respond will unfortunately ultimately progress on these therapies. Activation of ErbB3, the preferred dimerization partner of ErbB2, plays a key role in driving ErbB2-amplified tumor growth, but we have found that current ErbB2-directed therapies are poor inhibitors of ligand-induced activation. By simulating ErbB3 inhibition in a computational model of ErbB2/ErbB3 receptor signaling, we predicted that a bispecific antibody that docks onto ErbB2 and subsequently binds to ErbB3 and blocks ligand-induced receptor activation would be highly effective in ErbB2-amplified tumors, with superior activity to a monospecific ErbB3 inhibitor. We have developed a bispecific antibody suitable for both large scale production and systemic therapy by generating a single polypeptide fusion protein of two human scFv antibodies linked to modified human serum albumin. The resulting molecule, MM-111, forms a trimeric complex with ErbB2 and ErbB3, effectively inhibiting ErbB3 signaling and showing antitumor activity in preclinical models that is dependent on ErbB2 overexpression. MM-111 can be rationally combined with trastuzumab or lapatinib for increased antitumor activity and may in the future complement existing ErbB2-directed therapies to treat resistant tumors or deter relapse. *Mol Cancer Ther; 11(3); 1–12. ©2012 AACR.*

## Introduction

The family of cell surface ErbB receptors, ErbB1–4, play an essential role in development and physiology, mediating cellular growth and differentiation in multiple tissues, both in the developing embryo and in the adult (1). Escape of ErbB-activated pathways from normal control mechanisms results in tumorigenesis and growth (1). A prominent example is the amplification and overexpression of ErbB2 that occurs in 20% to 30% of breast and gastric carcinomas. Although lacking a high affinity ligand ErbB2 efficiently propagates prosurvival signals by forming heterodimers with other ErbB family members such as ErbB3. Therapeutic agents targeting ErbB2 (2), have greatly improved outcomes for many patients with ErbB2-overexpressing tumors but a significant proportion do not benefit and initial responders often develop resistance (3). ErbB3 activation following engagement of its ligand, heregulin, can mediate resistance to ErbB-targeted therapies (4–8). ErbB3 expression is upregulated in trastuzumab resistant tumor cells (9) and associated with poor prognosis in breast cancer (10, 11). Despite lacking an active kinase domain ErbB3 forms heterodimers with other members of the ErbB family to generate robust cellular signals through activation of the phosphoinositide 3-kinase (PI3K) pathway. ErbB3 is a preferred dimerization partner of ErbB2 (12, 13) and the ErbB2/ErbB3 heterodimer has been identified as the most potent activator of AKT compared to other ErbB receptor heterodimers with a strong dependence on ErbB3 for maintenance of oncogenic signaling (14, 15). However, as ErbB3 lacks an active kinase domain and does not become amplified or significantly overexpressed in tumors, ErbB2 has largely

**Authors' Affiliation:** Merrimack Pharmaceuticals, Cambridge, Massachusetts

**Note:** Supplementary material for this article is available at Molecular Cancer Therapeutics Online (http://mct.aacrjournals.org/).

C.F. McDonagh, A. Huhalov, and B.D. Harms contributed equally to this work.

Current address for J. Gu: Abbott Bioresearch Center, Worcester, Massachusetts 01605; and current address for M.J. Feldhaus, Adimab, 16 Cavendish Ct, Lebanon, New Hampshire 03753.

**Corresponding Author:** Ulrik B. Nielsen, Merrimack Pharmaceuticals, One Kendall Square, Suite B7201, Cambridge, MA 02139. Phone: 617-441-1006; Fax: 617-491-1386; E-mail: unielsen@merrimackpharma.com

**doi:** 10.1158/1535-7163.MCT-11-0820

Published OnlineFirst January 16, 2012; DOI: 10.1158/1535-7163.MCT-11-0820



remained the major therapeutic target in this heterodimeric oncogenic unit.

Recently, a computational analysis of the ErbB signaling network identified ErbB3 as the principal perpetrator of PI3K activation following ligand engagement (16). These data support direct therapeutic targeting of ErbB3 and subsequently an anti-ErbB3 antibody, MM-121, was developed that shows potent AKT inhibition and attenuation of tumor growth (16, 17). Traditionally, ErbB-mediated tumor growth was thought to arise through dependence of tumor cells on a mutated or amplified receptor, as exemplified by ErbB1 and ErbB2, respectively. These data generated by Schoeberl and colleagues (16) support an additional emerging paradigm of ErbB-dependent tumor growth through a combinatorial ligand-induced mechanism without the requirement for receptor overexpression or mutation. In the case of ErbB2-amplified tumors it seems that both oncogenic addiction and ligand activation may combine to drive potent aberrant signaling through the ErbB2/ErbB3 heterodimer and combinations of targeted therapies may be required for optimal antitumor activity.

In this study, we show that the approved ErbB2-targeted therapies, trastuzumab and lapatinib, are poor inhibitors of ligand-induced ErbB3 activation in ErbB2-overexpressing tumor cells. Likewise, pertuzumab, a monoclonal antibody in clinical development that binds to the extracellular ErbB2 dimerization domain, cannot effectively suppress ligand-induced ErbB3 phosphorylation. Thus, we have extended the mathematical ErbB network modeling approach described by Schoeberl and colleagues (16) to guide the design of an optimal inhibitor of the ligand activated ErbB2/ErbB3 oncogenic unit in ErbB2-overexpressing tumor cells. These simulations predicted that a bispecific molecule that targets the ErbB2/ErbB3 heterodimer and promotes the formation of inactive trimeric complexes is more effective at inhibiting ErbB3 activation than either an ErbB2 or ErbB3 monoclonal antibody. Consequently, we have developed MM-111, a bispecific antibody fusion protein consisting of fully human anti-ErbB2 and anti-ErbB3 single chain antibody moieties linked by modified human serum albumin (HSA). MM-111 binds with both avidity and specificity to tumor cells expressing ErbB2 and ErbB3 and blocks ligand-induced signaling and tumor growth in several preclinical models.

Trastuzumab was recently shown to effectively inhibit basal ErbB3 signaling in the absence of ligand stimulation (18). However, in agreement with our findings, trastuzumab did not effectively block ligand-induced activation of ErbB2/ErbB3 signaling thus providing tumor cells with an escape mechanism from trastuzumab therapy (18). ErbB3 may also provide escape from lapatinib therapy, which causes ErbB3 upregulation in both preclinical models and patient samples following treatment (19). We hypothesized that the combined inhibition of ErbB2 and ErbB3 provided by addition of MM-111 to either trastuzumab or lapatinib would synergistically inhibit tumor cell growth. Indeed, we report here that such combinations are effective and concurrent treatment of MM-111 and an ErbB2-targeted agent may deter resistance through ErbB3 activation.

## Materials and Methods

### Cell lines, cell culture conditions, cloning, and protein production

Cell lines were obtained from American Type Culture Collection (ATCC) with the exception of BT-474-M3, provided by Dr. Daryl Drummond (Hermes Biosciences) and NCI/ADRr, obtained from the NCI. All cell lines were passaged for fewer than 6 months after resuscitation, and purchased cell lines were cultured using the protocol provided. To obtain the BT-474-M3 cell line, BT-474 cells, obtained from ATCC, were passaged twice through mice with the fastest growing 2 tumors out of 10 selected for *ex vivo* propagation during each round of selection. Tumors were excised and cultured *ex vivo* to obtain the M3 subline that was verified by single-nucleotide polymorphism analysis. MM-111 was subcloned downstream of the human glyceraldehydes-3-phosphate dehydrogenase promoter between 2 Matrix Attachment Region elements (20). HSA containing C34S and N503Q mutations was obtained by gene synthesis (Codon Devices). MM-111–binding variant MM-111ΔErbB2 was constructed by mutating amino acids in the CDR3 of the B1D2 $V_H$ domain, and variant MM-111ΔErbB3 was constructed by replacing the H3 scFv with the mutated B1D2 scFv. MM-111, MM-111ΔErbB2, and MM-111ΔErbB3 were stably expressed in CHO-K1 cells in shake flasks or 10 L WAVE bags and purified from conditioned media by Blue Sepharose chromatography. The extracellular domain of human ErbB2 was expressed in CHO-K1 cells as a *histidine*-tagged fusion protein and purified by nickel affinity chromatography. Pertuzumab was produced as described previously (16). Trastuzumab was obtained from pharmacy. Lapatinib was obtained by custom synthesis (Biomol International). ErbB3 extracellular domain Fc fusion protein (ErbB3ecd-Fc) and heregulin 1-β were obtained from R&D Systems. The H3 scFv was cloned into the pCYN bacterial expression vector and expressed in *Escherichia coli* as a *histidine*-tagged fusion protein.

### Computational design of MM-111

A computational model of heregulin-induced p-ErbB3 signaling, as well as models of the inhibitors pertuzumab and lapatinib, were used as previously described (16). For format simulations, computational models were constructed according to the following reactions:

***ErbB2/3-bispecific antibody.***

$$E2 + BsAb \leftrightarrow E2{:}BsAb \quad (A)$$
$$BsAb + E3 \leftrightarrow BsAb{:}E3 \quad (B)$$
$$E2 + BsAb{:}E3 \leftrightarrow E2{:}BsAb{:}E3 \quad (C)$$
$$E2{:}BsAb + E3 \leftrightarrow E2{:}BsAb{:}E3 \quad (D)$$

Published OnlineFirst January 16, 2012; DOI: 10.1158/1535-7163.MCT-11-0820



*ErbB2 monoclonal antibody*

$$E2 + IgG \leftrightarrow E2{:}IgG \quad (E)$$
$$E2{:}IgG + E2 \leftrightarrow E2{:}IgG{:}E2 \quad (F)$$

*ErbB3 monoclonal antibody*

$$E3 + IgG \leftrightarrow E3{:}IgG \quad (G)$$
$$E3{:}IgG + E3 \leftrightarrow E3{:}IgG{:}E3 \quad (H)$$

Interaction parameters between each inhibitor arm and its target were $k_{on} = 10^5$ $(M\ s)^{-1}$ and $k_{off} = 10^{-3}$ $(s^{-1})$. Reactions (C), (D), (F), and (H) represent avid inhibitor binding leading to receptor cross-linking; for these reactions, all inhibitors were assumed to have equal cross-linking potency. For format simulations, assumed receptor levels were ErbB1 = 0, ErbB2 = $10^6$/cell, and ErbB3 = $4 \times 10^4$/cell. Simulated conditions were 24-hour preincubation of inhibitor followed by 10 minutes of 5 nmol/L heregulin stimulation. All computations were conducted in MATLAB 7.7 (The MathWorks).

### *In vitro* signaling studies

*In vitro* signaling experiments were carried out as described previously (16). Briefly, serum-starved cells were preincubated with MM-111, pertuzumab, trastuzumab, lapatinib, or combinations followed by stimulation with 5 nmol/L heregulin 1-β (R&D Systems) for 10 minutes. p-ErbB3 and p-AKT were measured by ELISA as described previously (16). Inhibitor $IC_{50}$ values were calculated by fitting dose–response data to a 4-parameter sigmoidal curve (GraphPad Prism). As appropriate, computational and experimental data for ligand-induced signaling were compared by subtraction of the unstimulated control and normalization to maximum observed signal.

### Receptor profiling and binding studies

ErbB1, ErbB2, and ErbB3 receptor levels were determined by quantitative FACS as described previously (16). ErbB3 scFv H3 blocking of heregulin/ErbB3 binding was assessed in a BIAcore. Heregulin was coupled to a CM5 sensor chip, and 50 nmol/L ErbB3ecd-Fc in HBS alone or mixed with 500 nmol/L H3 scFv or 500 nmol/L control IgG (C225) was flowed over the chip. To measure cell-binding affinities, MALME-3M cells (1,00,000 per well) were seeded into a 96-well plate and MM-111, MM-111ΔErbB2, and MM-111ΔErbB3 was added at concentrations indicated. Cells were then incubated with a 1:500 dilution of Alexa 647–labeled (Invitrogen) goat anti-HSA antibody (Bethyl Laboratories) and stained with 0.5 μg/mL propidium iodide followed by FACS analysis.

### Cell proliferation assays

Cells were incubated overnight following seeding, and inhibitor was added for 24 hours (lapatinib) or 6 days (MM-111, trastuzumab, pertuzumab, or combinations). For experiments with ligand stimulation, cells were serum-starved overnight before addition of inhibitor and 2 nmol/L heregulin 1-β was added 1 hour postinhibitor treatment in media containing 5% FBS. Cell viability was measured by the CellTiter-Glo Luminescent Cell Viability Assay (Promega).

### Cell-cycle analysis

BT-474-M3 cells (1,00,000 per well) were plated into a 6-well plate and the following day 1 μmol/L MM-111 was added for 72 hours. Cells were treated with propidium iodide and RNAse A and cell-cycle distribution was measured by FACS.

### Western blotting to determine inhibition of cyclin D1

BT-474-M3 cells were treated with MM-111 for 72 hours and then lysed with RIPA buffer (Sigma-Aldrich) supplemented with protease and phosphatase inhibitor cocktails (Roche). Cell lysate proteins were resolved by SDS-PAGE, and immunoblots were probed with rabbit anti-cyclin D1 antibody (Thermo Fisher).

### p27 immunohistochemistry

For p27 staining, BT-474-M3 cells (40,000) were seeded on glass coverslips and incubated with 1 μmol/L MM-111 for 6 hours. Fixed and permeabilized cells were blocked and then incubated with mouse anti-p27 antibody (BD Biosciences).

### MM-111 serum stability and pharmacokinetic analysis

MM-111 was incubated in mouse serum (Sigma-Aldrich) at 37°C for 120 hours. Samples were removed and MM-111 was detected by a bispecificity ELISA. Briefly, a 96-well plate was coated with ErbB2ecd domain overnight followed by blocking (Pierce) and incubation with MM-111. Plates were then incubated with Fc-ErbB3 followed by goat anti-human-Fc-HRP conjugate (Jackson ImmunoResearch). To determine the stability of MM-111 in circulation 5- to 6-week-old female CD-1 nude mice (Charles River Labs) were dosed with 30 mg/kg MM-111 by bolus intravenous injection. Serum was harvested 0.5, 4, 8, 24, 48, 72, and 120 hours postinjection and MM-111 was detected by an HSA ELISA (Bethyl Laboratories) and the bispecificity ELISA.

### Xenograft efficacy studies

Tumor xenografts were established by subcutaneous injection of tumor cells into the flanks of 5- to 6-week-old female athymic nude mice (*nu/nu*; Charles River Laboratories) except for MDA-MB-361 cells that were injected into 5- to 6-week-old female nonobese diabetic/severe combined immunodeficient (NOD/SCID) mice (Charles River Laboratories). For the BT-474-M3 and ZR75-1 models, mice received a subcutaneous 60-day, slow-release estrogen implant in the opposite flank (0.72 mg pellet; Innovation Research of America), 24 hours before the injection of cells. Once

Published OnlineFirst January 16, 2012; DOI: 10.1158/1535-7163.MCT-11-0820



tumors reached a mean volume of 150 to 500 $mm^3$, mice were randomized into groups of 8 or 10 and dosed by intraperitoneal injection.

## Results

### A bispecific antibody approach is optimal for inhibiting ErbB3 in ErbB2-overexpressing cells

We conducted inhibitor dose–response assays to investigate the ability of the ErbB2-directed therapies, lapatinib, trastuzumab, and pertuzumab to inhibit p-ErbB3 in heregulin-stimulated BT-474-M3 cells that overexpress ErbB2 (Table 1). We found that all 3 molecules weakly inhibited ErbB3 phosphorylation with $IC_{50}$ values of 96 and 260 nmol/L for pertuzumab and lapatinib, respectively (Fig. 1A), whereas trastuzumab was unable to inhibit heregulin-induced ErbB3 activation. We then applied a previously developed computational model of heregulin-induced signaling of the ErbB receptor signaling network (16) to explore optimal inhibitor formats for specifically disrupting signaling through the ErbB2/3 heterodimer in ErbB2-overexpressing cells. The protein–protein interactions, biochemical reactions, and kinetic parameters incorporated into the model are described by Schoeberl and colleagues (16). To validate the model, we generated *in silico* representations of lapatinib and pertuzumab ErbB3 inhibition, which compared accurately with experimental data (Fig. 1A).

We next created *in silico* models of 3 paradigms for inhibiting signaling from the ErbB2/ErbB3 heterodimer: an ErbB2 monoclonal antibody, an ErbB3 monoclonal, and an ErbB2/3-bispecific antibody. The inhibition of ErbB3-mediated signaling by the *in silico* ErbB2 antibody occurs through sequestration of ErbB2 receptors from ErbB3, thereby preventing the formation of ErbB2/3 heterodimers. In contrast, the ErbB3 antibody and ErbB2/3 bispecific antibody function by blocking heregulin binding to ErbB3. To isolate the role of inhibitor format in driving the efficacy of ErbB3 inhibition, these generic inhibitor models used identical kinetic binding parameters [$k_{on} = 10^5\ (M\ s)^{-1}$ and $k_{off} = 10^{-3}\ (s^{-1})$] and ability to bivalently cross-link their targets. The relative ability to inhibit ligand-induced ErbB3 phosphorylation was simulated in a model cell expressing $1 \times 10^6$ ErbB2 receptors per cell and $4 \times 10^4$ ErbB3 receptors per cell under 5 nmol/L heregulin stimulation. In this model system our simulations suggest that an ErbB2/3-bispecific antibody offers superior p-ErbB3 $IC_{50}$ potency (0.2 nmol/L) compared with either an ErbB2 ($IC_{50}$ = 58 nmol/L) or ErbB3 ($IC_{50}$ = 3.1 nmol/L) monoclonal antibody. Moreover, the bispecific antibody is more

**Table 1.** ErbB1, ErbB2, and ErbB3 receptors per cell for tumor cell lines and p-ErbB3 $IC_{50}$ values and percentage of inhibition values following MM-111 treatment

| | | Receptors/cell[a] | | | p-ErbB3 $IC_{50}$, nmol/L[c] | p-ErbB3 % inhibition[d] |
|---|---|---|---|---|---|---|
| Cell line[b] | Tumor | ErbB1 | ErbB2 | ErbB3 | Mean (SD) | Mean (SD) |
| Receptor measurement with signaling analysis | | | | | | |
| ADRr | Ovarian | 177,818 | 40,792 | 33,205 | 8.50 (2.12) | 43 (15.56) |
| LS180 | Colon | 122,520 | 143,339 | 28,841 | 0.53 (0.21) | 68 (17.52) |
| ZR75-1 | Breast | 37,409 | 199,132 | 39,492 | 0.89 (0.58) | 87 (13.72) |
| MDA-MB361 | Breast | 65,855 | 371,731 | 32,981 | 0.77 (0.04) | 94 (0.14) |
| ADRr-E2 | Ovarian | 271,000 | 722,000 | 34,400 | 1.1 (0.12) | 94 (1.26) |
| NCI-N87 | Gastric | 417,753 | 1,233,479 | 34,678 | 5.70 (3.82) | 109 (22.63) |
| BT-474-M3 | Breast | 129,436 | 1,706,601 | 49,238 | 2.60 (2.83) | 115 (9.90) |
| ZR75-30 | Breast | 3,091 | 2,395,485 | 43,897 | 0.65 (0.78) | 94 (1.41) |
| Receptor measurements | | | | | | |
| ACHN | Renal | 448,284 | 45,456 | 15,200 | | |
| MALME-3M | Melanoma | 2,914 | 56,422 | 67,367 | | |
| IGROV1 | Ovarian | 149,031 | 158,418 | 5,355 | | |
| CALU-3 | Lung | 161,357 | 1,196,976 | 30,031 | | |
| SKOV3 | Ovarian | 264,132 | 1,377,661 | 13,694 | | |

[a]The levels of ErbB1, ErbB2, and ErbB3 receptors per cell were measured by quantitative FACS. Values reported are a mean of at least 2 experiments.

[b]Cell lines are ordered according to ErbB2 expression levels.

[c]p-ErbB3 $IC_{50}$ values were assessed by ELISA in cell lysates from serum-starved cells treated with MM-111 for 24 hours followed by stimulation with 5 nmol/L heregulin. Data shown are a mean of more than 2 replicates and were analyzed by fitting dose–response data to a 4-parameter sigmoidal curve (GraphPad Prism) to provide $IC_{50}$ values.

[d]The percentage of p-ErbB3 inhibition is the maximal inhibition observed normalized to the maximum observed signal (100%) and the basal unstimulated signal (0%).

Published OnlineFirst January 16, 2012; DOI: 10.1158/1535-7163.MCT-11-0820



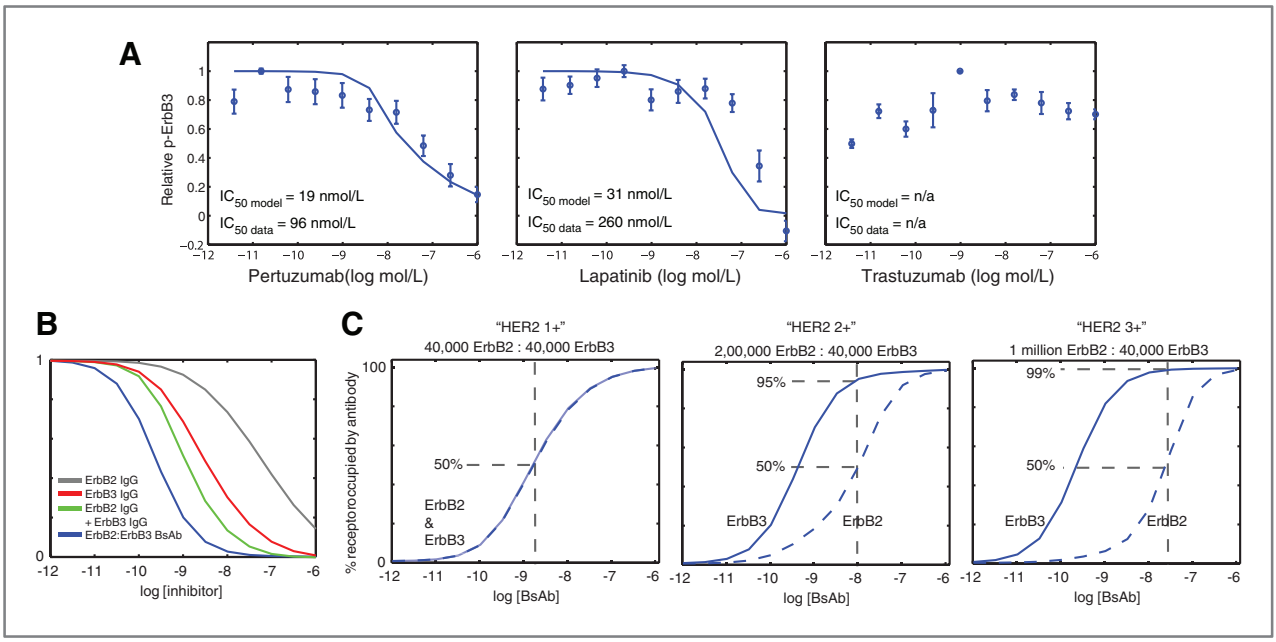


Figure 1. Rational design of an optimized inhibitor of ligand-activated ErbB3 in ErbB2-overexpressing cells. A, a dose range of pertuzumab, lapatinib, or trastuzumab was applied to BT-474-M3 cells followed by stimulation with 5 nmol/L heregulin. p-ErbB3 was then measured by ELISA. Model-generated dose–response curves overlay the experimental data. B, simulations of heregulin-activated p-ErbB3 inhibition by an ErbB2 IgG, ErbB3 IgG, ErbB2 IgG, and ErbB3 IgG combination and an ErbB2/ErbB3-bispecific antibody in a model cell expressing $1 \times 10^6$ ErbB2 receptors per cell. C, the percentage of occupancy of ErbB2 and ErbB3 by MM-111 was assessed in model cells with equal expression of ErbB2 and ErbB3 ($4 \times 10^4$ receptors per cell; "HER2 1+"), overexpression of ErbB2 to levels of $2 \times 10^5$ ("HER2 2+") and $1 \times 10^6$ ("HER2 3+").

potent than a combination of both ErbB2 and ErbB3 antibodies ($IC_{50} = 1.1$ nmol/L; Fig. 1B).

Using simulations of on-cell binding, we further explored the relative ability of a bispecific antibody to bind to ErbB3 receptors in cells with different levels of ErbB2. In model cells with equal expression of ErbB2 and ErbB3 ($4 \times 10^4$ receptors per cell; "HER2 1+"), 50% receptor occupancy of ErbB2 results in 50% occupancy of ErbB3 by the bispecific antibody. However, simulated overexpression of ErbB2 to levels of $2 \times 10^5$ (corresponding to an immunohistochemistry score of approximately "HER2 2+") and $1 \times 10^6$ (corresponding to an immunohistochemistry score of approximately "HER2 3+") receptors per cell led to increasingly strong occupancy of ErbB3 receptor to 95% and 99%, respectively. These results predicted that an ErbB2/3-bispecific antibody would potently target ErbB3 only in cells overexpressing ErbB2 (Fig. 1C).

## Engineering and production of MM-111 and MM-111 binding variants

The ErbB2 and ErbB3 scFv binding arms, B1D2 and H3, respectively, were chosen for building MM-111. The ErbB2 scFv component of MM-111, B1D2 (21), is an affinity matured version of the C6.5 scFv (22) that binds receptor with an affinity of 0.3 nmol/L (Supplementary Fig. S1A) providing ErbB2 targeting, whereas the ErbB3 scFv component of MM-111, H3 (23), binds to ErbB3 with an affinity of 16 nmol/L (Supplementary Fig. S1B). Both the B1D2 scFv and H3 scFv bind specifically to ErbB2 and ErbB3, respectively, and do not interact with other ErbB family members (Supplementary Fig. S2). We investigated the ability of the H3 scFv to block heregulin binding to ErbB3. Preincubation of ErbB3ecd-Fc with H3 scFv prevented binding of ErbB3ecd-Fc to heregulin immobilized on a CM5 chip (Fig. 2A and B). A mutated variant of HSA, mHSA, was inserted between the H3 and B1D2 scFvs of MM-111 with short connector peptide linkers, AAS and AAAL, inserted at the amino and carboxyl terminus of mHSA, respectively. The long serum half-life of HSA of approximately 21 days has been reported to be due to its recycling by the FcRn receptor by a similar mechanism to IgG recycling (24) and incorporating HSA into therapeutic biologics is an established strategy for enhancing serum half-life. To achieve greater homogeneity of the HSA linker, we made 2 point mutations. A cysteine residue at position 34 of native HSA was mutated to serine to reduce potential protein heterogeneity due to oxidation at this site. An asparagine residue at amino acid 503 of native HSA, which in native HSA is sensitive to deamidation, was mutated to glutamine. Analysis of purified MM-111 and its variants MM-111ΔErbB2 and MM-111ΔErbB3 by size exclusion chromatography showed that greater than 95% of each purified protein eluted in the monomeric fraction (Supplementary Fig. S3).

## Formation of a trimeric complex of MM-111 bound to both ErbB2 and ErbB3 is required for potent ErbB3 antagonism

The ability of MM-111 to bind cells avidly by engaging both ErbB2 and ErbB3 was tested on the melanoma

Published OnlineFirst January 16, 2012; DOI: 10.1158/1535-7163.MCT-11-0820



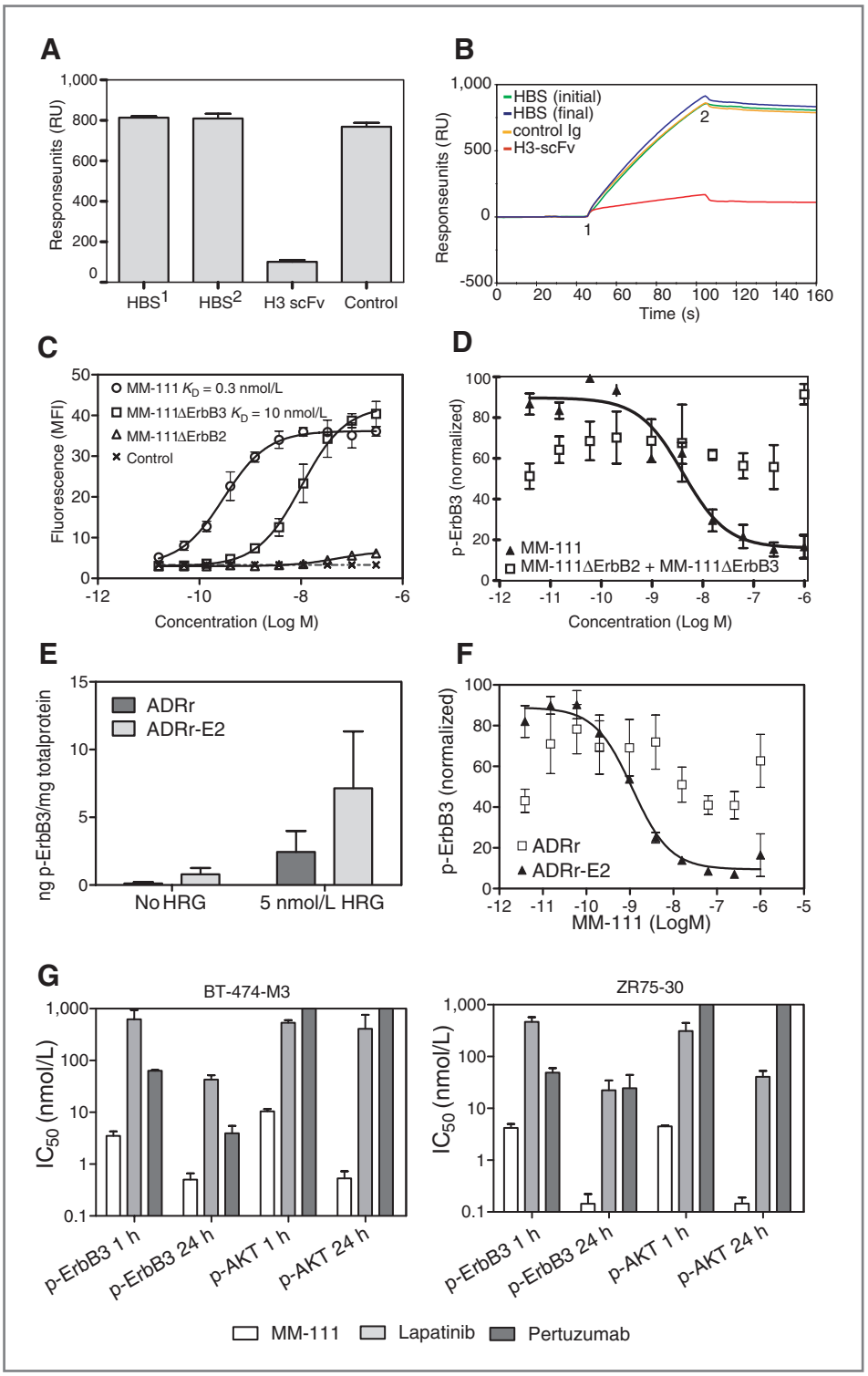


**Figure 2.** Inhibition of ErbB3 signaling and tumor growth by formation of a trimeric MM-111/ErbB2/ErbB3 complex. A, fifty nanomolar ErbB3ecd-Fc mixed with 500 nmol/L H3-scFv, 500 nmol/L control IgG, or HBS (HBS[1], initial injection; HBS[2], final injection) were passed over a heregulin-coupled sensor chip in a BIAcore. Maximum response units are shown averaged for 2 experiments (B). Representative sensorgram data (A). B, 1, injection of ErbB3ecd-Fc mixed with H3-scFv, control IgG, or HBS over heregulin-coupled sensor chip and beginning of association phase. 2, end of association phase and beginning of disassociation phase. C, a dose range of MM-111, MM-111ΔErbB3, or MM-111ΔErbB2 was incubated with MALME-3M melanoma cells followed by FACS analysis to determine the apparent binding affinity of each molecule. D, MM-111 or a combination of MM-111ΔErbB3 and MM-111ΔErbB2 were incubated with BT-474-M3 cells for 24 hours followed by stimulation with heregulin, and p-ErbB3 was measured by ELISA. Data are normalized to unstimulated control. Model simulations overlay experimental data. E, both basal and heregulin-stimulated levels of p-ErbB3 were compared in the parental ADRr cells and ADRr cells stably transfected with ErbB2 and ADRr-E2. F, the parental ADRr cells and ADRr-E2 transfectants were treated for 24 hours with a dose range of MM-111 followed by stimulation with heregulin, and p-ErbB3 was measured by ELISA. Data are normalized to unstimulated control. G, BT-474-M3 and ZR75-30 cells were incubated with a dose range of MM-111, pertuzumab, or lapatinib for 1 and 24 hours followed by heregulin stimulation, and p-ErbB3 and p-AKT $IC_{50}$ values were determined.

tumor cell line Malme-3M, which expresses approximately equivalent levels of the 2 receptors as determined using quantitative FACS methods (Table 1), thus allowing assessment of binding avidity. Although the ErbB3 scFv component of MM-111, H3, specifically binds ErbB3 and blocks heregulin (Fig. 2A and B) incubation of MM-111ΔErbB2, which lacks ErbB2 binding activity, with Malme-3M cells resulted in no measurable cell binding (Fig. 2C), likely due to its monovalent affinity of 16 nmol/L. MM-111ΔErbB3, which retains a functional, high affinity ErbB2 binding scFv but lacks ErbB3 binding activity had an apparent $K_D$

Published OnlineFirst January 16, 2012; DOI: 10.1158/1535-7163.MCT-11-0820



of 10 nmol/L (Fig. 2C). MM-111 bound cells with an apparent $K_D$ of 0.3 nmol/L showing avidity binding of greater than 30-fold than the single binding arms (Fig. 2C) and indicating that MM-111 interacts with ErbB2 and ErbB3 simultaneously. A dose–response experiment on BT-474-M3 cells showed that following 24 hours incubation MM-111 potently inhibits ErbB3 phosphorylation, with an $IC_{50}$ value of 3 nmol/L, whereas a combination of MM-111ΔErbB2 and MM-111ΔErbB3 providing an equivalent dose of ErbB2 and ErbB3 binding moieties is ineffective (Fig. 2D). Together these data show that MM-111 is a potent inhibitor of p-ErbB3 in ErbB2-overexpressing cells and inhibition requires simultaneous binding of both ErbB2 and ErbB3 receptors by MM-111 to form a trimeric inhibitory complex.

We subsequently assessed MM-111 potency on a panel of tumor cell lines expressing a range of ErbB2 levels. We observed that $IC_{50}$ values for p-ErbB3 inhibition were consistently in the low nanomolar range, regardless of ErbB2 expression level, but the ability of MM-111 to inhibit ligand-activated p-ErbB3 to basal levels was strongly positively correlated with ErbB2 expression levels (Table 1). To further investigate the dependency of MM-111 activity on ErbB2 levels we examined the potency of MM-111 in ovarian ADRr cells, expressing $4 \times 10^4$ ErbB2 receptors per cell and an ErbB2-overexpressing transfectant of ADRr, ADRr-E2, which express $7 \times 10^5$ ErbB2 receptors per cell. We observed a 3-fold increase in heregulin-stimulated p-ErbB3 levels in the ADRr-E2 cells compared with the parental ADRr line (Fig. 2E). Despite this, elevation in ErbB3 activation MM-111 displayed far greater potency and percentage of inhibition of p-ErbB3 in the ADRr-E2 cell line relative to the parent ADRr cells showing the specificity of MM-111 for the ErbB2/ErbB3 oncogenic unit in tumor cells overexpressing ErbB2 receptors (Fig. 2F).

## MM-111 potently inhibits the PI3K pathway and proliferation of ErbB2-overexpressing tumor cells

Potent inhibition of ErbB3 phosphorylation was achieved in BT-474-M3 ($IC_{50} = 3$ nmol/L) cells and an additional ErbB2-overexpressing breast tumor cell line, ZR75-30 ($IC_{50} = 5$ nmol/L; Fig. 2G) following 1 hour incubation with MM-111. In addition, we observed inhibition by MM-111 of p-AKT in BT-474-M3 ($IC_{50} = 10$ nmol/L) and in ZR75-30 ($IC_{50} = 4$ nmol/L; Fig. 2G). We found that the ability of MM-111 to inhibit heregulin-induced ErbB3 activation was superior to lapatinib and pertuzumab (Fig. 2G) and the relative $IC_{50}$ value for each inhibitor was consistent following up to 24 hours incubation with inhibitors, indicating treatment times had little effect on the potency of the inhibitors (Fig. 2G). Despite moderately inhibiting ErbB3 phosphorylation, pertuzumab did not effectively inhibit AKT whereas lapatinib was a poor inhibitor (Fig. 2G). Consistent with our earlier observations (Fig. 1A), trastuzumab was found to be an ineffective inhibitor of ligand-induced ErbB3 and AKT phosphorylation following 1- and 24-hour treatment in both cell lines tested (data not shown).

## MM-111 is active in circulation and inhibits tumor growth in xenograft models

MM-111 is a fusion protein with multiple components, including unnatural peptide linkers. Although proteolytic resistance was a criterion for selecting connector peptides for MM-111, we wished to confirm the stability and proteolytic resistance of MM-111 both *in vitro* and in circulation. First, we incubated MM-111 in serum at a predicted therapeutic dose of 100 nmol/L and investigated its stability over a 5-day time course. MM-111 retained its ability to bind both recombinant ErbB2 and ErbB3 when incubated in mouse (Fig. 3A) and human (Supplementary Fig. S4) serum at 37°C with similar activity for all time points compared with the 0 hour control. MM-111 also remained stable in circulation in mice with comparable serum levels of MM-111 measured by an HSA assay and an assay that measured active circulating levels of MM-111 that retain simultaneous interaction with both ErbB2 and ErbB3 (Fig. 3B). We also measured the serum levels of MM-111 in mice administered 5, 15, and 45 mg/kg of bispecific antibody. Pharmacokinetic data were subjected to noncompartmental analysis to estimate the terminal half-life. Nude mice dosed with 5, 15, 30, or 45 mg/kg had similar terminal half lives of 16.6, 16.2, 22.6, and 17.5 hours, respectively (Supplementary Table S1).

MM-111 efficacy *in vivo* was initially investigated in the BT-474-M3 breast tumor xenograft model. HSA was administered as a control at an equimolar concentration to MM-111. Statistical significance was observed between HSA and 30 and 3 mg/kg MM-111 treatment groups from days 8 and 14, respectively (Fig. 3C). The 0.3 mg/kg MM-111 treatment group was not significantly different from HSA treatment (Fig. 3C). To thoroughly investigate the relationship between MM-111 antitumor activity and ErbB2 expression levels, MM-111 was studied in a panel of 9 models (ADRr, ACHN, IGROV1, ZR-75-1, MDA-MB-361, ADRr-E2, Calu-3, NCI-N87, and SK-OV-3) expressing a range of ErbB2 from $4.0 \times 10^4$ to $1.4 \times 10^6$ receptors per cell (Table 1) that showed relative MM-111 activity was dependent on ErbB2 overexpression (Fig. 3D). The ADRr-E2 xenograft model of the ErbB2-overexpressing engineered cell line derived from ADRr cells responded well to MM-111 treatment whereas the parental ADRr xenografts did not respond to MM-111 (Fig. 3D). This observation in xenografts of ADRr-E2 transfectants is consistent with the inhibition of ErbB3 phosphorylation we observe *in vitro* (Fig. 2F).

## MM-111 induces antiproliferative effects in tumors

The effect of MM-111 on the accumulation of BT-474 cells in $G_1$ phase and the concomitant decrease in S-phase of the cell cycle was examined. MM-111 modestly

Published OnlineFirst January 16, 2012; DOI: 10.1158/1535-7163.MCT-11-0820



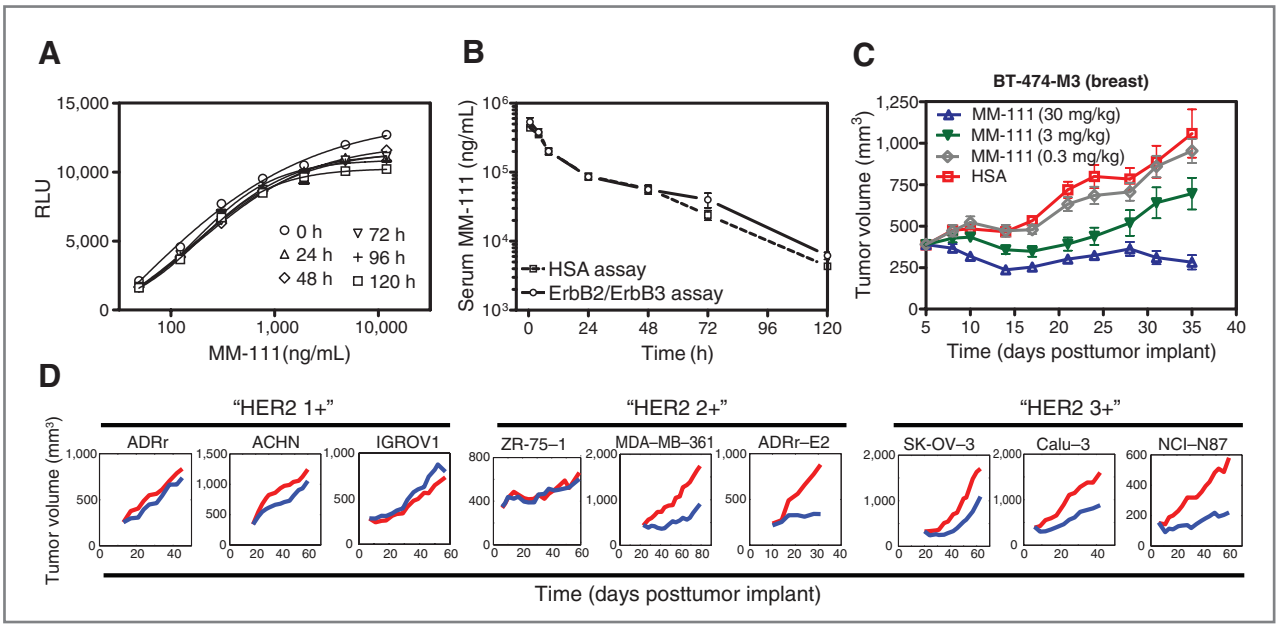


Figure 3. MM-111 is stable under physiologic conditions and has potent antitumor activity *in vivo*. A, MM-111 was incubated in mouse serum at 37°C. Aliquots were removed at 24-hour intervals, and the ability of MM-111 to interact with both ErbB2 and ErbB3 antigens was assessed by a sandwich assay. B, MM-111 stability was evaluated in nude mice administered a single 30 mg/kg intravenous dose of MM-111. Serum was analyzed for the presence of MM-111 by 2 distinct assays. The HSA assay measured levels of HSA present in mouse serum, whereas the ErbB2/ErbB3 assay assessed levels of active circulating MM-111. C, the *in vivo* efficacy of MM-111 was determined in xenograft models of BT-474-M3 at the doses indicated. HSA was dosed at 17 mg/kg, an equimolar dose to 30 mg/kg MM-111. D, the activity of MM-111 was investigated in a panel of xenograft models (ADRr, ACHN, IGROV1, ZR-75-1, MDA-MB-361, ADRr-E2, Calu-3, NCI-N87, and SK-OV-3) dosed with 30 mg/kg MM-111 every 3 days. Her2 immunohistochemistry scores approximated from quantitative FACS receptor measurements on cell lines are indicated for each xenograft. RLU, relative luminescence units.

decreased the percentage of cells in S-phase by 9.5% and the population of cells in $G_1$ phase increased by 11% (Fig. 4A). We subsequently examined the ability of MM-111 to inhibit signaling molecules downstream of ErbB3 that regulate cell-cycle progression or cell death. MM-111 downregulated cell-cycle modulator cyclin D1 (Fig. 4B) and induced nuclear translocation of cell-cycle inhibitor p27 in BT-474-M3 cells following 72 hours of treatment (Fig. 4C). Annexin V staining of BT-474-M3 cells treated with MM-111 did not show an apoptotic effect (data not shown).

## MM-111 combines favorably with trastuzumab or lapatinib to inhibit growth of ErbB2-overexpressing tumors

As MM-111 is a potent inhibitor of ligand-induced ErbB3 activation in ErbB2-overexpressing cancer cells, we hypothesized that its combination with ErbB2 inhibitors, trastuzumab or lapatinib, would have additive or synergistic effects on growth in tumors sensitive to both agents. First, we investigated the differential ability of MM-111, lapatinib, and trastuzumab to inhibit cell proliferation in the presence of heregulin. Under basal conditions, we

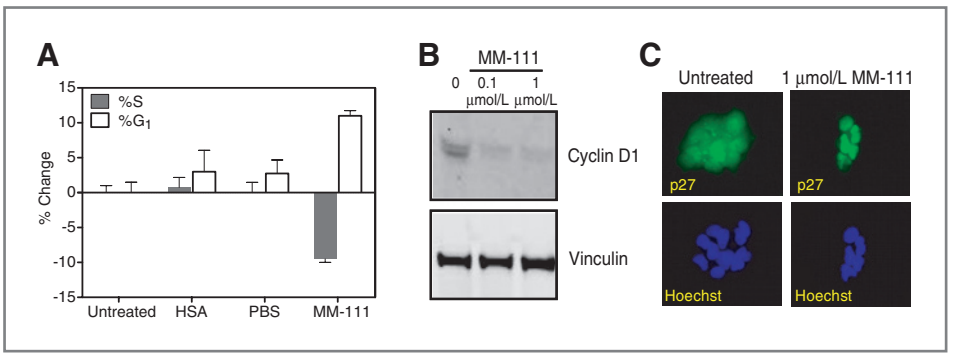


Figure 4. MM-111 exerts an antiproliferative effect on tumor cells. A, cell-cycle distribution in $G_1$ and S-phases was measured by flow cytometry in BT-474 cells treated with 1 μmol/L HSA or 1 μmol/L MM-111. B, BT-474-M3 cells treated with the indicated dose of MM-111 for 72 hours were harvested, washed, and lysed. Cell lysate proteins were resolved by SDS-PAGE and subjected to immunoblot analysis with an anti-cyclin D1 antibody. C, BT-474-M3 cells were treated with 1 μmol/L MM-111 or left untreated. Cells were fixed, and p27 distribution was assessed by staining with an anti-p27 antibody.

Published OnlineFirst January 16, 2012; DOI: 10.1158/1535-7163.MCT-11-0820



found that lapatinib, trastuzumab, and MM-111 maximally inhibit BT-474-M3 cell proliferation by 50%, 32%, and 24%, respectively (Fig. 5A). When cells are cultured in the presence of 5 nmol/L heregulin the effect of both lapatinib and trastuzumab is compromised, decreasing inhibition of cell proliferation to 23% and 9%, respectively (Fig. 5A). The inhibition of tumor cell growth by MM-111 is enhanced when heregulin is present, with 33% growth inhibition observed (Fig. 5A). This observation suggested that both lapatinib and trastuzumab may work additively in combination with an inhibitor of heregulin-driven signaling such as MM-111.

We next investigated the ability of the combination of MM-111 and lapatinib or MM-111 and trastuzumab to inhibit AKT phosphorylation. While we found that lapatinib alone inhibited p-AKT in the presence of heregulin the combination of MM-111 and lapatinib was extremely effective, inhibiting p-AKT well below basal levels at therapeutically relevant concentrations (Fig. 5B). Trastuzumab does not inhibit heregulin-activated ErbB2/3 signaling (Fig. 1A; ref. 18). However, as we increased combination doses of MM-111 and trastuzumab we observed improved p-AKT inhibition to basal levels suggesting an additive effect of the combination (Fig. 5B).

The combination of MM-111 with trastuzumab or lapatinib was further investigated *in vivo* using the BT-474-M3 breast cancer xenograft model. Suboptimal monotherapy doses of MM-111 (3 mg/kg dosed every 3 days; Fig. 3B) and trastuzumab (1 mg/kg dosed weekly) were selected for combination experiments to allow observation of any differences in activity between monotherapy and combination groups. Tumor growth inhibition in groups dosed with the combination of 3 mg/kg MM-111 and 1 mg/kg trastuzumab was more potent than the monotherapy-treated groups and on day 17 posttumor implantation reached statistical significance compared with MM-111 alone ($P = 1.4 \times 10^{-5}$) and trastuzumab alone ($P = 1.4 \times 10^{-7}$). MM-111 and lapatinib were each dosed at an optimal efficacious dose weekly and everyday, respectively. The combination of MM-111 and lapatinib provided more potency than either drug alone reaching statistical significance to MM-111 ($P = 3.9 \times 10^{-4}$) and lapatinib ($P = 5.1 \times 10^{-3}$) on day 13 (Fig. 5C).

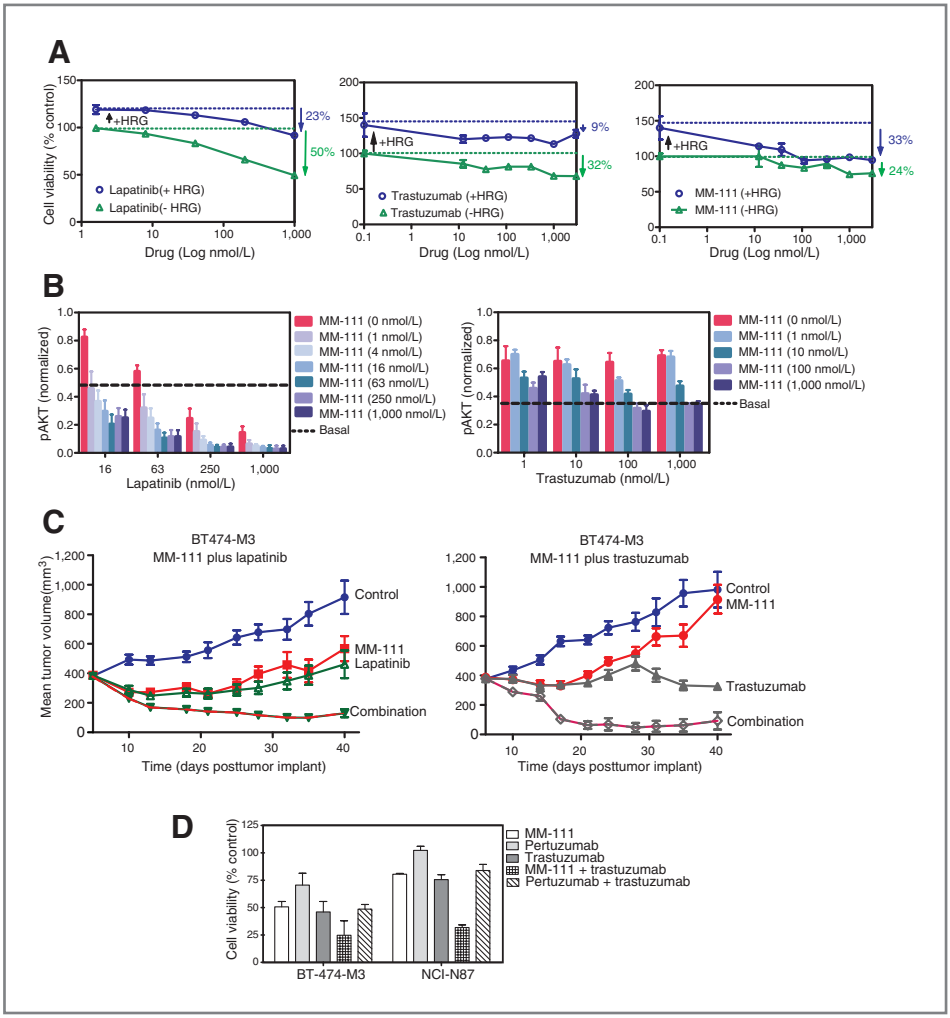


**Figure 5.** MM-111 positively combines with ErbB2-targeted agents to inhibit breast tumor growth. A, BT-474-M3 cells were treated with dose ranges of lapatinib, trastuzumab, or MM-111 in the presence or absence of 5 nmol/L heregulin. Viable cells were counted following 6 days of treatment. Data are normalized to unstimulated control. B, the effect of MM-111 combined with lapatinib or trastuzumab on p-AKT inhibition was assessed in heregulin-stimulated BT-474-M3 cells across a dose range. C, BT-474-M3 breast tumor xenograft models were treated with MM-111 (3 mg/kg every 3 days), trastuzumab (1 mg/kg every 7 days), or a combination of both drugs at these doses. In a separate experiment, BT-474-M3 breast tumor xenografts were treated with MM-111 (66 mg/kg every 7 days), lapatinib (150 mg/kg every day), or a combination of both drugs. D, BT-474-M3 or NCI-N87 cells were treated with 1 μmol/L MM-111, trastuzumab, pertuzumab, or the combination of MM-111 and trastuzumab or pertuzumab and trastuzumab in 10% serum. Viable cells were counted following 6 days of treatment. Data are normalized to unstimulated control.

Published OnlineFirst January 16, 2012; DOI: 10.1158/1535-7163.MCT-11-0820



The combination of trastuzumab and pertuzumab has been shown to be synergistic (25, 26). We compared the combination of MM-111 and trastuzumab to pertuzumab plus trastuzumab and found that the MM-111 combination was superior at inhibiting proliferation of both BT-474-M3 and NCI-N87 tumor cells (Fig. 5D). In addition, activity of MM-111 as a single agent was similar to trastuzumab and superior to pertuzumab in these models (Fig. 5D).

## Discussion

ErbB3 has been identified as a key node in the ligand-activated ErbB receptor PI3K signaling axis (16). Unlike ErbB1 and ErbB2, ErbB3 does not require adaptor proteins to interact with the regulatory p85 subunit of PI3K, instead interacting directly through up to 6 potential phosphotyrosines. Consequently, ErbB3 activation proficiently triggers PI3K signaling and activation of this pathway is frequently observed in tumors that escape from currently marketed ErbB-directed inhibitors (4, 6, 8, 27), as well as hormonal therapy (28, 29) and chemotherapy (30, 31). Thus, inhibition of ErbB3 activation by heregulin is a worthy therapeutic strategy that is being actively pursued (16, 17). However, in ErbB2-overexpressing tumors ErbB2/3 heterodimers preform in the absence of ligand to create a primed, picomolar-affinity binding site for heregulin that is several 100-fold higher in affinity than the ErbB3/heregulin interaction (32) and challenging for a subnanomolar affinity inhibitor to impede. MM-111 is designed to deliver ErbB3 inhibition through docking to the overexpressed ErbB2 receptor and overcomes the high affinity ErbB2/3/heregulin complex through enhanced apparent affinity for ErbB3 as a result of binding avidity. Computational modeling predicts that the bispecific design provides close to 100% occupancy of ErbB3 by MM-111 at therapeutically relevant doses in cells that overexpress ErbB2.

At nonamplified levels of ErbB2, ErbB3 occupancy by MM-111 is greatly reduced indicating that the bispecifc design also promotes tumor selectivity. Robinson and colleagues (33) have shown the superior tumor selectivity of a bispecific antibody with ALM, an ErbB2/ErbB3-bispecific antibody generated by linking an anti-ErbB2 scFv and anti-ErbB3 scFv with a synthetic peptide linker. Tumor-specific inhibition of ErbB2-targeted agents is desirable as ErbB2 plays a role in ensuring survival and growth of cardiomyocytes (34). Trastuzumab treatment has been shown to result in cardiac dysfunction due to left ventricular ejection fraction decline that becomes more prevalent with coadministered anthracyclines (35). Similar though less severe toxicities have occurred with lapatinib (36). We anticipate that the high specificity of MM-111 for tumor cells coexpressing ErbB2 and ErbB3 may prevent target-related toxicity in the clinic. To further mitigate against cardiotoxicity, we selected B1D2 as the anti-ErbB2 scFv moiety of MM-111 because it does not inhibit ErbB2 signaling (37).

The ErbB2/ErbB3-bispecific antibody, ALM, has shown antiproliferative activity on tumor cells *in vitro* (33) but with a molecular weight of approximately 55 kDa this protein is expected to have a short circulating half-life due to rapid renal clearance and thus is unlikely to achieve serum levels required for activity in patients. Others have found that using HSA as a linker between 2 scFvs can extend serum half-life significantly (38). We found that incorporating HSA between the H3 and B1D2 scFvs extended the serum half-life of MM-111 to 16 to 20 hours in mice compared with approximately 5 hours typically observed for tandem scFvs reported in the literature (39). In cynomolgus monkeys a circulating half-life of MM-111 of up to 99 hours was achieved (Supplementary Table S1), and we anticipate that MM-111 half lives in patients may exceed those observed in monkey as species compatibility is achieved.

The partition of signaling and kinase function to ErbB3 and ErbB2, respectively, presents significant challenges to inhibiting the ErbB2/ErbB3 heterodimer. Trastuzumab blocks ligand independent ErbB2/ErbB3 activation (18), but we show here that trastuzumab is an ineffective inhibitor of heregulin-activated ErbB2/3 signaling. Thus, when autocrine or paracrine heregulin is available tumor cells may continue to thrive under trastuzumab therapy. Indeed, heregulin expression is observed in the majority of primary breast tumors (40, 41) and is upregulated in preclinical ErbB2-overexpressing models following trastuzumab treatment (8, 42). Pertuzumab binds to the dimerization domain of ErbB2, blocking the formation of ligand-induced ErbB2/ErbB3 heterodimers, and a combination of pertuzumab and trastuzumab synergistically inhibits the survival of breast cancer cells (15, 25, 26). Although some of the activity of both trastuzumab and pertuzumab is mediated through antibody-dependent cell-mediated cytotoxicity, the synergistic activity of the combination is attributed to the complementary pathway inhibitory mechanisms of each antibody rather than their ability to recruit effector cells (26). The combination of trastuzumab and pertuzumab has achieved success in the clinic. A phase II trial in patients with Her2-positive metastatic breast cancer who had previously progressed on trastuzumab therapy achieved a 50% clinical benefit rate and 24.2% objective response rate (43). We show here that MM-111 inhibition of ligand-activated ErbB3 phosphorylation is superior to pertuzumab and the combination of MM-111 and trastuzumab is more effective at inhibiting tumor cell growth than pertuzumab plus trastuzumab. Pertuzumab indirectly inhibits ErbB3 activation by precluding ErbB2 dimerization whereas MM-111 binds directly to ErbB3 and blocks heregulin. As ErbB2 is expressed at an order of magnitude or greater than ErbB3, even a high percentage of ErbB2 inhibition still leaves enough free receptors to form active ErbB2/3 heterodimers. Ironically, this overexpression of ErbB2 in tumors makes it more difficult to inhibit with ErbB2-directed therapies in tumors relative to normal tissues. MM-111 on the other hand is potentiated by ErbB2

Published OnlineFirst January 16, 2012; DOI: 10.1158/1535-7163.MCT-11-0820



overexpression making this an attractive approach to tumor specific inhibition of receptor tyrosine kinases.

We found the addition of MM-111 to trastuzumab was very effective at inhibiting tumor growth, observing a significant combination effect in the BT-474 breast tumor model *in vitro* and *in vivo*, and it is possible that the combination of MM-111 and trastuzumab could offer benefit to Her2-positive patients whose tumors escape trastuzumab therapy through heregulin activation of ErbB3. Lapatinib reversibly inhibits the kinase activity of ErbB1 and ErbB2 and while lapatinib, unlike trastuzumab, can perturb heregulin-activated ErbB3 phosphorylation, MM-111 is far more effective and the activity of lapatinib is attenuated by heregulin. ErbB3 upregulation in lapatinib-treated patients (19) indicates that concurrent ErbB3 inhibition is desirable and we found that addition of MM-111 to lapatinib increased p-AKT suppression and weekly MM-111 added to daily lapatinib administration improved tumor growth inhibition *in vivo*. Interestingly, we did not observe an improvement in antitumor activity in xenografts when daily lapatinib dosing was combined with MM-111 dosed every 3 days suggesting that the dosing schedule or sequence of administration of these 2 agents may be critical for activity and warrants further investigation.

In conclusion, we have used computational modeling and cell signaling insights to develop an engineered antibody fusion molecule, MM-111, that potently and specifically inhibits ErbB3 signaling in ErbB2-positive tumors by exploiting the overexpression of ErbB2 through incorporation of a bispecific design. As the critical role of ErbB3/heregulin activation in ErbB2-positive refractory disease unravels the stage is set for the clinical development of MM-111, a specialized ErbB3 inhibitor that can act in concert with ErbB2 therapies to deter resistance or restore sensitivity.

## Disclosure of Potential Conflicts of Interest

All authors were employees of Merrimack Pharmaceuticals with ownership interests in the company at the time this work was undertaken.

## Acknowledgments

The authors thank Gege Tan and Maja Razlog for excellent technical assistance and Drs. James Marks, Louis Weiner, and Clet Niyikiza for helpful discussions.

The costs of publication of this article were defrayed in part by the payment of page charges. This article must therefore be hereby marked *advertisement* in accordance with 18 U.S.C. Section 1734 solely to indicate this fact.

Received November 3, 2011; accepted January 3, 2012; published OnlineFirst January 16, 2012.

## References

1. Yarden Y, Sliwkowski MX. Untangling the ErbB signalling network. Nat Rev Mol Cell Biol 2001;2:127–37.
2. Baselga J, Swain SM. Novel anticancer targets: revisiting ERBB2 and discovering ERBB3. Nat Rev Cancer 2009;9:463–75.
3. Nahta R, Yu D, Hung MC, Hortobagyi GN, Esteva FJ. Mechanisms of disease: understanding resistance to HER2-targeted therapy in human breast cancer. Nat Clin Pract Oncol 2006;3:269–80.
4. Huang X, Gao L, Wang S, McManaman JL, Thor AD, Yang X, et al. Heterotrimerization of the growth factor receptors erbB2, erbB3, and insulin-like growth factor-I receptor in breast cancer cells resistant to Herceptin. Cancer Res 2010;70:1204–14
5. Motoyama AB, Hynes NE, Lane HA. The efficacy of ErbB receptor-targeted anticancer therapeutics is influenced by the availability of epidermal growth factor-related peptides. Cancer Res 2002;62:3151–8.
6. Sergina NV, Rausch M, Wang D, Blair J, Hann B, Shokat KM, et al. Escape from HER-family tyrosine kinase inhibitor therapy by the kinase-inactive HER3. Nature 2007;445:437–41.
7. Engelman JA, Cantley LC. The role of the ErbB family members in non-small cell lung cancers sensitive to epidermal growth factor receptor kinase inhibitors. Clin Cancer Res 2006;12:4372s–6s.
8. Gijsen M, King P, Perera T, Parker PJ, Harris AL, Larijani B, et al. HER2 phosphorylation is maintained by a PKB negative feedback loop in response to anti-HER2 herceptin in breast cancer. PLoS Biol 2011;8:e1000563.
9. Narayan M, Wilken JA, Harris LN, Baron AT, Kimbler KD, Maihle NJ. Trastuzumab-induced HER reprogramming in "resistant" breast carcinoma cells. Cancer Res 2009;69:2191–4.
10. Sassen A, Rochon J, Wild P, Hartmann A, Hofstaedter F, Schwarz S, et al. Cytogenetic analysis of HER1/EGFR, HER2, HER3 and HER4 in 278 breast cancer patients. Breast Cancer Res 2008;10:R2.
11. Witton CJ, Reeves JR, Going JJ, Cooke TG, Bartlett JM. Expression of the HER1-4 family of receptor tyrosine kinases in breast cancer. J Pathol 2003;200:290–7.
12. Graus-Porta D, Beerli RR, Daly JM, Hynes NE. ErbB-2, the preferred heterodimerization partner of all ErbB receptors, is a mediator of lateral signaling. Embo J 1997;16:1647–55.
13. Tzahar E, Waterman H, Chen X, Levkowitz G, Karunagaran D, Lavi S, et al. A hierarchical network of interreceptor interactions determines signal transduction by Neu differentiation factor/neuregulin and epidermal growth factor. Mol Cell Biol 1996;16:5276–87.
14. Holbro T, Beerli RR, Maurer F, Koziczak M, Barbas CF III, Hynes NE. The ErbB2/ErbB3 heterodimer functions as an oncogenic unit: ErbB2 requires ErbB3 to drive breast tumor cell proliferation. Proc Natl Acad Sci U S A 2003;100:8933–8.
15. Lee-Hoeflich ST, Crocker L, Yao E, Pham T, Munroe X, Hoeflich KP, et al. A central role for HER3 in HER2-amplified breast cancer: implications for targeted therapy. Cancer Res 2008;68:5878–87.
16. Schoeberl B, Pace EA, Fitzgerald JB, Harms BD, Xu L, Nie L, et al. Therapeutically targeting ErbB3: a key node in ligand-induced activation of the ErbB receptor-PI3K axis. Sci Signal 2009;2:ra31.
17. Sheng Q, Liu X, Fleming E, Yuan K, Piao H, Chen J, et al. An activated ErbB3/NRG1 autocrine loop supports *in vivo* proliferation in ovarian cancer cells. Cancer Cell 2010;17:298–310.
18. Junttila TT, Akita RW, Parsons K, Fields C, Lewis Phillips GD, Friedman LS, et al. Ligand-independent HER2/HER3/PI3K complex is disrupted by trastuzumab and is effectively inhibited by the PI3K inhibitor GDC-0941. Cancer Cell 2009;15:429–40.
19. Garrett JT, Olivares MG, Rinehart C, Granja-Ingram ND, Sanchez V, Chakrabarty A, et al. Transcriptional and posttranslational up-regulation of HER3 (ErbB3) compensates for inhibition of the HER2 tyrosine kinase. Proc Natl Acad Sci U S A 2011;108:5021–6.
20. Zahn-Zabal M, Kobr M, Girod PA, Imhof M, Chatellard P, de Jesus M, et al. Development of stable cell lines for production or regulated expression using matrix attachment regions. J Biotechnol 2001;87:29–42.
21. Schier R, McCall A, Adams GP, Marshall KW, Merritt H, Yim M, et al. Isolation of picomolar affinity anti-c-erbB-2 single-chain Fv by

Published OnlineFirst January 16, 2012; DOI: 10.1158/1535-7163.MCT-11-0820



molecular evolution of the complementarity determining regions in the center of the antibody binding site. J Mol Biol 1996;263:551–67.
22. Schier R, Marks JD, Wolf EJ, Apell G, Wong C, McCartney JE, et al. *In vitro* and *in vivo* characterization of a human anti-c-erbB-2 single-chain Fv isolated from a filamentous phage antibody library. Immunotechnology 1995;1:73–81.
23. Horak E, Heitner T, Robinson MK, Simmons HH, Garrison J, Russeva M, et al. Isolation of scFvs to *in vitro* produced extracellular domains of EGFR family members. Cancer Biother Radiopharm 2005;20:603–13.
24. Chaudhury C, Mehnaz S, Robinson JM, Hayton WL, Pearl DK, Roopenian DC, et al. The major histocompatibility complex-related Fc receptor for IgG (FcRn) binds albumin and prolongs its lifespan. J Exp Med 2003;197:315–22.
25. Nahta R, Hung MC, Esteva FJ. The HER-2-targeting antibodies trastuzumab and pertuzumab synergistically inhibit the survival of breast cancer cells. Cancer Res 2004;64:2343–6.
26. Scheuer W, Friess T, Burtscher H, Bossenmaier B, Endl J, Hasmann M. Strongly enhanced antitumor activity of trastuzumab and pertuzumab combination treatment on HER2-positive human xenograft tumor models. Cancer Res 2009;69:9330–6.
27. Engelman JA, Zejnullahu K, Mitsudomi T, Song Y, Hyland C, Park JO, et al. MET amplification leads to gefitinib resistance in lung cancer by activating ERBB3 signaling. Science 2007;316:1039–43.
28. Frogne T, Benjaminsen RV, Sonne-Hansen K, Sorensen BS, Nexo E, Laenkholm AV, et al. Activation of ErbB3, EGFR and Erk is essential for growth of human breast cancer cell lines with acquired resistance to fulvestrant. Breast Cancer Res Treat 2009;114:263–75.
29. Liu B, Ordonez-Ercan D, Fan Z, Edgerton SM, Yang X, Thor AD. Downregulation of erbB3 abrogates erbB2-mediated tamoxifen resistance in breast cancer cells. Int J Cancer 2007;120:1874–82.
30. Knuefermann C, Lu Y, Liu B, Jin W, Liang K, Wu L, et al. HER2/PI-3K/Akt activation leads to a multidrug resistance in human breast adenocarcinoma cells. Oncogene 2003;22:3205–12.
31. Wang S, Huang X, Lee CK, Liu B. Elevated expression of erbB3 confers paclitaxel resistance in erbB2-overexpressing breast cancer cells via upregulation of Survivin. Oncogene 2010;29:4225–36.
32. Fitzpatrick VD, Pisacane PI, Vandlen RL, Sliwkowski MX. Formation of a high affinity heregulin binding site using the soluble extracellular domains of ErbB2 with ErbB3 or ErbB4. FEBS Lett 1998;431:102–6.
33. Robinson MK, Hodge KM, Horak E, Sundberg AL, Russeva M, Shaller CC, et al. Targeting ErbB2 and ErbB3 with a bispecific single-chain Fv enhances targeting selectivity and induces a therapeutic effect *in vitro*. Br J Cancer 2008;99:1415–25.
34. Pugatsch T, Abedat S, Lotan C, Beeri R. Anti-erbB2 treatment induces cardiotoxicity by interfering with cell survival pathways. Breast Cancer Res 2006;8:R35.
35. Jerian S, Keegan P. Cardiotoxicity associated with paclitaxel/trastuzumab combination therapy. J Clin Oncol 1999;17:1647–8.
36. Perez EA, Koehler M, Byrne J, Preston AJ, Rappold E, Ewer MS. Cardiac safety of lapatinib: pooled analysis of 3689 patients enrolled in clinical trials. Mayo Clin Proc 2008;83:679–86.
37. Neve RM, Nielsen UB, Kirpotin DB, Poul MA, Marks JD, Benz CC. Biological effects of anti-ErbB2 single chain antibodies selected for internalizing function. Biochem Biophys Res Commun 2001;280:274–9.
38. Muller D, Karle A, Meissburger B, Hofig I, Stork R, Kontermann RE. Improved pharmacokinetics of recombinant bispecific antibody molecules by fusion to human serum albumin. J Biol Chem 2007;282:12650–60.
39. Holliger P, Hudson PJ. Engineered antibody fragments and the rise of single domains. Nat Biotechnol 2005;23:1126–36.
40. Hutcheson IR, Knowlden JM, Hiscox SE, Barrow D, Gee JM, Robertson JF, et al. Heregulin beta1 drives gefitinib-resistant growth and invasion in tamoxifen-resistant MCF-7 breast cancer cells. Breast Cancer Res 2007;9:R50.
41. Revillion F, Lhotellier V, Hornez L, Bonneterre J, Peyrat JP. ErbB/HER ligands in human breast cancer, and relationships with their receptors, the bio-pathological features and prognosis. Ann Oncol 2008;19:73–80.
42. Ritter CA, Perez-Torres M, Rinehart C, Guix M, Dugger T, Engelman JA, et al. Human breast cancer cells selected for resistance to trastuzumab *in vivo* overexpress epidermal growth factor receptor and ErbB ligands and remain dependent on the ErbB receptor network. Clin Cancer Res 2007;13:4909–19.
43. Baselga J, Gelmon KA, Verma S, Wardley A, Conte P, Miles D, et al. Phase II trial of pertuzumab and trastuzumab in patients with human epidermal growth factor receptor 2-positive metastatic breast cancer that progressed during prior trastuzumab therapy. J Clin Oncol 2010;28:1138–44.

Published OnlineFirst January 16, 2012; DOI: 10.1158/1535-7163.MCT-11-0820



Molecular Cancer Therapeutics

# Antitumor Activity of a Novel Bispecific Antibody That Targets the ErbB2/ErbB3 Oncogenic Unit and Inhibits Heregulin-Induced Activation of ErbB3

Charlotte F. McDonagh, Alexandra Huhalov, Brian D. Harms, et al.

*Mol Cancer Ther* Published OnlineFirst January 16, 2012.